D J Med Sci 2026;12(1):20-35
doi: 10.5606/fng.btd.2026.239

Original Article

Dysregulated expression patterns of hsa-miR-9-5p and hsa-let-7a-5p are associated with altered NFAT5, ARID1A, and ZFP36 expression in NSCLC cell lines

Yağız Turan Kızılkaya, Perisu Yıldız Ünal

Department of Molecular Biology and Genetics, Demiroğlu Bilim University Faculty of Arts and Sciences, İstanbul, Türkiye

ABSTRACT

Objectives: This study aimed to evaluate the expression patterns of hsa-miR-9-5p and hsa-let-7a-5p together with nuclear factor of activated T-cells 5 (NFAT5), AT-rich interacting domain-containing protein 1A (ARID1A), and zinc finger protein 36 (ZFP36) in non-small cell lung cancer (NSCLC) cell lines and to externally contextualize these findings using ENCORI/starBase transcriptomic data.

Materials and methods: The A549 and H1299 NSCLC cell lines and the non-tumorigenic bronchial epithelial BEAS-2B cell line were cultured under standard conditions. Total ribonucleic acid (RNA), including small RNA fractions, was isolated and converted into complementary deoxyribonucleic acid for microRNA (miRNA) and messenger RNA (mRNA) analyses. Quantitative real-time polymerase chain reaction (qRT-PCR) analyses were performed using SYBR Green chemistry. qRT-PCR was performed to determine the expression levels of hsa-miR-9-5p, hsa-let-7a-5p, NFAT5, ARID1A, and ZFP36. U6 and glyceraldehyde-3-phosphate dehydrogenase were used as endogenous controls for miRNA and mRNA analyses, respectively. Relative expression was calculated using the 2-ΔΔCt method, and statistical analyses were performed using ΔCt values. ENCORI/starBase was used to examine tumor-normal expression patterns and miRNA-mRNA co-expression relationships in lung adenocarcinoma (LUAD) and lung squamous cell carcinoma (LUSC) cohorts.

Results: The hsa-miR-9-5p expression was significantly increased in A549 and H1299 cells compared with BEAS-2B cells, whereas hsa-let-7a-5p expression was significantly reduced. NFAT5 expression was markedly upregulated in both NSCLC cell lines, while ARID1A and ZFP36 expression levels were decreased, particularly in A549 cells. ENCORI/starBase analyses partially supported the *in vitro* findings, showing higher hsa-miR-9-5p expression and lower hsa-let-7a-5p and ZFP36 expression in lung cancer samples. Co-expression analysis further showed a weak but significant inverse correlation between hsa-miR-9-5p and ZFP36 in both LUAD and LUSC.

Conclusion: The findings demonstrate a coordinated expression profile in NSCLC cell lines characterized by increased hsa-miR-9-5p and NFAT5 expression together with reduced hsa-let-7a-5p, ARID1A, and ZFP36 expression. ENCORI/starBase data provide external support, particularly for the hsa-miR-9-5p/ZFP36 relationship. However, these findings should be interpreted as association-level evidence, and further functional studies are required to validate direct miRNA-mRNA regulatory interactions.

Keywords: ARID1A, ENCORI, hsa-let-7a-5p, hsa-miR-9-5p, NFAT5, ZFP36.

Lung cancer (LC) remains the leading cause of cancer-related mortality worldwide, with an estimated 1.8 million deaths in 2022.[1] Non-small cell lung cancer (NSCLC) represents the major histological category of LC and includes lung adenocarcinoma (LUAD), lung squamous cell carcinoma (LUSC), and large-cell carcinoma as its principal subtypes. Although molecularly targeted therapies and immune checkpoint inhibitors have improved outcomes in selected patient groups, metastatic progression, tumor heterogeneity, and treatment resistance continue to limit durable clinical responses.[2] Defining regulatory molecular networks that coordinate oncogenic activation and tumor-suppressive loss in NSCLC, therefore, remains both biologically and clinically relevant.

Micro-ribonucleic acids (miRNAs) are small non-coding RNAs of approximately

Received: May 20, 2026
Accepted: May 25, 2026
Published online: June 09, 2026

Correspondence: Yağız Turan Kızılkaya.
E-mail: yagizturankizilkaya@gmail.com

Cite this article as:
Kızılkaya YT, Yıldız Ünal P. Dysregulated expression patterns of hsa-miR-9-5p and hsa-let-7a-5p are associated with altered NFAT5, ARID1A, and ZFP36 expression in NSCLC cell lines. D J Med Sci 2026;12(1):20-35. doi: 10.5606/fng.btd.2026.239.

22 nucleotides that regulate gene expression predominantly through post-transcriptional repression of target messenger RNAs (mRNAs).[3] In cancer, miRNAs may function as either oncogenic or tumor-suppressive miRNAs, depending on cellular context, target repertoire, and disease stage.[4] In LC, altered miRNA expression has been associated with proliferation, invasion, epithelial plasticity, inflammatory signaling, and therapeutic resistance, supporting the biological relevance of miRNA-mRNA regulatory axes in NSCLC pathogenesis.[5]

Among miRNAs implicated in NSCLC, hsa-miR-9-5p has increasingly been described as an oncogenic miRNA, although its effects may vary depending on tumor context and target selection. Zhu et al.[6] showed that miR-9-5p promotes LUAD cell proliferation, migration, and invasion by directly targeting inhibitor of DNA binding 4 (ID4). Similarly, Li et al.[7] reported that miR-9-5p enhances NSCLC cell growth and metastatic behavior by repressing transforming growth factor beta receptor 2 (TGFBR2). More recently, Zhang et al.[8] demonstrated by reverse transcription-quantitative polymerase chain reaction (RT-qPCR) that miR-9-5p is upregulated in NSCLC tissues and cell lines compared with non-malignant controls and is associated with malignant clinicopathological features, including tumor size, lymphatic metastasis, and invasive capacity. These findings support an oncogenic role for miR-9-5p in NSCLC models.[6-8]

In contrast, the let-7 family is among the most established tumor-suppressive miRNA families in LC. Reduced let-7 expression has been reported in human LCs and is associated with shortened postoperative survival.[9] Mechanistically, let-7 family members regulate key oncogenic drivers, including rat sarcoma (RAS), and restoration of let-7 activity has been shown to suppress NSCLC tumor development in preclinical models.[10,11] These data provide a rationale for evaluating hsa-let-7a-5p in combination with an oncogenic miRNA, such as hsa-miR-9-5p, in NSCLC cell models.

The functional consequences of miRNA dysregulation depend strongly on the biological identity of their target mRNAs. Nuclear factor of activated T-cells 5 (NFAT5), AT-rich interacting domain-containing protein 1A (ARID1A), and zinc finger protein 36 (ZFP36) represent mechanistically distinct candidate mRNAs relevant to NSCLC biology. The NFAT5 is an osmosensitive and stress-responsive transcription factor implicated in LC progression. Guo and Jin[12] showed that NFAT5 is upregulated in LUAD cells and promotes proliferation and migration, in part by regulating aquaporin 5 expression. More recent evidence indicates that NFAT5 can regulate interleukin 8 and contribute to NSCLC cell growth, migration, and nuclear factor kappa B-related signaling.[13] These findings support NFAT5 as a pro-tumorigenic factor in LC.[12,13]

The ARID1A, a core component of the switch/sucrose-non-fermentable (SWI/SNF) chromatin-remodeling complex, has a contrasting tumor-suppressive role in LUAD. Loss of ARID1A expression has been shown to promote LUAD cell proliferation, migration, invasion, and metastasis and to predict poor prognosis.[14] Multi-omics analyses further indicate that ARID1A deficiency can enhance cell-cycle progression, activate oncogenic receptor tyrosine kinase signaling, and contribute to resistance to epidermal growth factor receptor (EGFR) tyrosine kinase inhibitors in EGFR-mutant LUAD.[15] Reduced ARID1A expression in NSCLC may therefore reflect loss of chromatin-dependent tumor-suppressive regulation with implications for metastasis and treatment resistance.

The ZFP36, also known as tristetraprolin, is an adenine-uracil (AU)-rich element-binding RNA-binding protein that promotes degradation of target mRNAs and is widely regarded as a post-transcriptional tumor suppressor.[16] In NSCLC, Zhang et al.[17] demonstrated that ZFP36 mediates the destabilization of BARX homeobox 1 (BARX1) mRNA. Loss of ZFP36 increased BARX1 expression and promoted proliferation, migration, invasion, and tumorigenicity by activating oncogenic programs involving cell division cycle 20 (CDC20), cell division cycle 45 (CDC45), tripartite motif-containing 37 (TRIM37), and matrix metalloproteinase-9 (MMP-9). These findings place ZFP36 within a post-transcriptional tumor-suppressive axis relevant to NSCLC progression.

Based on this background, the present study characterized the basal expression relationship between two functionally opposing miRNAs, hsa-miR-9-5p and hsa-let-7a-5p, and three mechanistically distinct candidate mRNAs: NFAT5, a stress-responsive and pro-tumorigenic transcription factor; ARID1A, a chromatin-remodeling tumor suppressor; and ZFP36, a post-transcriptional RNA-binding tumor suppressor involved in mRNA decay regulation. These candidates were selected based on their biological relevance to NSCLC-associated regulatory reprogramming and their potential involvement in miRNA-associated transcriptional and post-transcriptional dysregulation pathways. The BEAS-2B cells were used as a non-tumorigenic bronchial epithelial reference, whereas A549 and H1299 served as NSCLC models. To externally contextualize the *in vitro* findings, the Encyclopedia of RNA Interactomes (ENCORI)/starBase Pan-Cancer transcriptomic and miRNA-mRNA co-expression analyses were performed in LUAD and LUSC cohorts. Since the study design relied on baseline expression profiling rather than miRNA gain- or loss-of-function approaches, the findings were interpreted as association-level evidence rather than direct proof of miRNA-mRNA regulatory interactions.

MATERIALS AND METHODS

Cell lines and culture conditions

The human NSCLC cell lines A549 and H1299, along with the immortalized non-tumorigenic human bronchial epithelial cell line BEAS-2B, were utilized. All cell lines were obtained from the American Type Culture Collection (ATCC, Manassas, VA, USA). BEAS-2B functioned as the non-tumorigenic reference, whereas A549 and H1299 were used as NSCLC models.

Cells were cultured at 37°C in a humidified incubator with 5% carbon dioxide (CO_2). The A549 and H1299 were maintained in high-glucose Dulbecco's modified Eagle's medium (DMEM) (Gibco, Thermo Fisher Scientific, Grand Island, NY, USA, cat no: 11965092) supplemented with 10% heat-inactivated fetal bovine serum (Gibco, Thermo Fisher Scientific, Grand Island, NY, USA, Cat no: A5670801) 1% penicillin-streptomycin (Gibco, Thermo Fisher Scientific, Grand Island, NY, USA, Cat no: 15140122). The BEAS-2B cells were cultured under identical conditions to enable comparative analysis. Cells were passaged prior to reaching confluence and harvested for RNA isolation at 80-90% confluence. Independent biological replicates were included for each cell line. Cells were seeded in six-well plates and harvested for RNA isolation at the designated confluence. Cell lines were routinely monitored for mycoplasma contamination using PCR-based quality-control procedures. Only cultures exhibiting normal morphology and adequate viability were selected for qRT-PCR analysis.

RNA isolation

Total RNA, including small RNA fractions, was isolated from BEAS-2B, A549, and H1299 cells using the miRNeasy Tissue/Cells Advanced Mini Kit (217604, Qiagen, Hilden, Germany) following the manufacturer's instructions. After washing with phosphate-buffered saline (Gibco, Thermo Fisher Scientific, Grand Island, NY, USA, cat no: 10010023), cells were lysed, and RNA was purified using a spin-column extraction method.

The RNA concentration and purity were assessed using a NanoDrop spectrophotometer (Thermo Fisher Scientific, Inc., Waltham, MA, USA). Only samples with acceptable A260/A280 and A260/A230 ratios were selected for complementary DNA (cDNA) synthesis. The RNA samples were stored at -80°C until further analysis.

cDNA synthesis

Complementary DNA synthesis was conducted separately for miRNA and mRNA

Table 1. Reverse transcription reaction components for miRNA analysis

Component	Quantity (µL)
RT reaction buffer (5X)	2
RNase-free water	5
RT enzyme mix	1
Template RNA	2
Total	10

RT, reaction buffer; miRNA, micro-ribonucleic acid.

analyses. For miRNA quantification, cDNA was synthesized from total RNA using the miRCURY LNA RT2 First Strand Kit (Qiagen, Hilden, Germany, cat no: 330404) in accordance with the manufacturer's protocol, as shown in Table 1. This cDNA was used to quantify hsa-miR-9-5p and hsa-let-7a-5p. For mRNA quantification, cDNA was synthesized using the RT^2 First Strand Kit (Qiagen, Hilden, Germany), following the manufacturer's instructions. Briefly, genomic DNA was first eliminated by incubating total RNA with genomic DNA elimination buffer at 37°C for 5 min. Reverse transcription was subsequently performed by adding BC5 reverse transcriptase mix to a final reaction volume of 20 µl, followed by incubation at 42°C for 15 min and enzyme inactivation at 95°C for 5 min. This cDNA was used to quantify ARID1A, NFAT5, and ZFP36.

Quantitative real-time PCR analysis

Quantitative real-time PCR was conducted using SYBR Green detection (Qiagen, Hilden, Germany, cat no: 330620) on a Rotor-Gene Q system (Qiagen, Hilden, Germany), as shown in Table 2. Validated gene-specific primers were employed for target miRNAs and mRNAs, as shown in Table 3. The U6 small nuclear RNA served as the endogenous control for miRNA analysis, while GAPDH was used as the endogenous control for mRNA analysis. The BEAS-2B cells functioned as the calibrator for relative expression.

Polymerase chain reactions were performed in technical triplicate. The protocol consisted of an initial denaturation at 95°C for 10 min, followed by 40 cycles of 95°C for 15 sec and 60°C for 60 sec. Melt-curve analysis was conducted to confirm product specificity and to exclude non-specific amplification or primer-dimer formation.

Table 2. qPCR reaction components for miRNA and mRNA analysis

Component	Quantity (µL)
qPCR mastermix (2×)	10
RNase-free water (ddH_2O)	6
RT^2 qPCR primer assay or miRCURY LNA miRNA PCR assay	1
Template RNA (1:10 diluted)	3
Total	20

qPCR, quantitative polymerase chain reaction; miRNA, micro-ribonucleic acid; RT, reverse transcription.

Table 3. Primer assay information for miRNA and mRNA expression analysis

Target	GeneGlobe ID	Accession number
hsa-miR-9-5p	YP00204513	MIMAT0000441
hsa-let-7a-5p	YP00205727	MIMAT0000062
ARID1A	PPH13453B	NM_006015
NFAT5	PPH01474B	NM_006599
ZFP36	PPH17294C	NM_003407
GAPDH	PPH00150F	NM_002046
U6	U6snRNA	YP02119464

miRNA, micro-ribonucleic acid.

Bioinformatic analysis using ENCORI/starBase

To complement the *in vitro* qRT-PCR findings, external transcriptomic evidence was evaluated using the ENCORI/starBase Pan-Cancer Analysis Platform.[18] ENCORI/starBase Pan-Cancer analyses were conducted using the Cancer Genome Atlas (TCGA)-derived transcriptomic datasets available on the ENCORI/starBase platform. Expression profiles for tumor and normal tissues in the LUAD and LUSC cohorts were retrieved directly from the database. Analyses used unmatched tumor and normal sample groups rather than paired samples from the same patients. Expression values, including log2(FPKM + 0.01) for mRNAs and log2(RPM + 0.01) for miRNAs, were used as provided by the ENCORI/starBase platform without additional recalculation. The miRNA-mRNA co-expression relationships were evaluated using the correlation analysis tools integrated within the ENCORI/starBase database, based on TCGA-associated transcriptomic datasets. The platform was queried for hsa-miR-9-5p, hsa-let-7a-5p, ARID1A, NFAT5, and ZFP36 in LUAD and LUSC cohorts.

Tumor-normal expression patterns were examined using ENCORI-generated box plots. For mRNA expression analysis, ARID1A, NFAT5, and ZFP36 were evaluated in LUAD cohorts comprising 526 cancer and 59 normal

samples and in LUSC cohorts comprising 501 cancer and 49 normal samples. For miRNA expression analysis, hsa-miR-9-5p and hsa-let-7a-5p were evaluated in LUAD cohorts comprising 512 cancer and 20 normal samples and in LUSC cohorts comprising 475 cancer and 38 normal samples.

Gene expression values were presented as log2(FPKM + 0.01), whereas miRNA expression values were presented as log2(RPM + 0.01), as provided by ENCORI/starBase. In addition, miRNA-mRNA co-expression relationships were examined using ENCORI-generated scatter plots for hsa-miR-9-5p and hsa-let-7a-5p against ARID1A, NFAT5, and ZFP36 in LUAD and LUSC cohorts. Correlation coefficients and p-values were recorded directly from the ENCORI/starBase output.

These analyses were used as external transcriptomic support for the *in vitro* findings and were not interpreted as direct evidence of miRNA-mRNA binding or functional repression.

Statistical analysis

Statistical analyses were performed using ΔCt values in GraphPad Prism version 10.0 (GraphPad Software, San Diego, CA, USA). Data are presented as mean ± SEM unless otherwise specified. For each target, one-way ANOVA followed by Dunnett's multiple-comparison test was applied, with BEAS-2B serving as the control group. A p-value of < 0.05 was considered statistically significant. Significance levels were indicated as follows: * $p < 0.05$, ** $p < 0.01$, *** $p < 0.001$.

For ENCORI/starBase analyses, tumor-normal expression profiles and miRNA-mRNA co-expression results were interpreted using the platform's statistical outputs. Correlation strength was evaluated based on the reported correlation coefficient (r) and corresponding p-value.

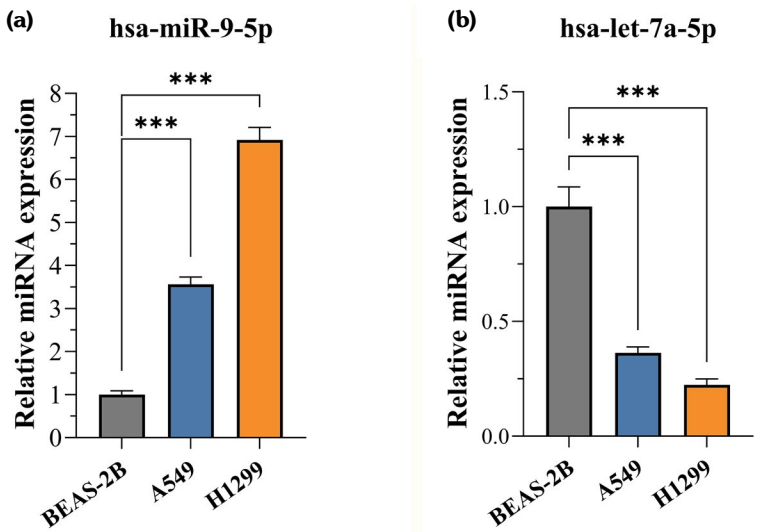

Figure 1. Relative expression levels of hsa-miR-9-5p and hsa-let-7a-5p in BEAS-2B, A549, and H1299 cells. Relative expression levels of hsa-miR-9-5p **(a)** and hsa-let-7a-5p **(b)** were analyzed by qRT-PCR. The U6 was used as the endogenous control, and BEAS-2B cells were used as the calibrator. Relative expression was calculated using the 2^-ΔΔCt method. The hsa-miR-9-5p expression was significantly increased in A549 and H1299 cells compared with BEAS-2B, whereas hsa-let-7a-5p expression was significantly reduced in both cancer cell lines.

Data are presented as mean ± SEM. Statistical comparisons were performed using one-way ANOVA followed by Dunnett's multiple comparisons test against BEAS-2B. *** $p < 0.001$ *vs.* BEAS-2B.

RESULTS

Basal expression of hsa-miR-9-5p and hsa-let-7a-5p in NSCLC cell lines

The basal expression levels of hsa-miR-9-5p and hsa-let-7a-5p were evaluated in BEAS-2B, A549, and H1299 cells by qRT-PCR. BEAS-2B cells served as the non-tumorigenic bronchial epithelial reference, and U6 was used as the endogenous control for miRNA normalization. Relative expression was calculated using the 2-ΔΔCt method.[19] Comparisons were performed using one-way ANOVA followed by Dunnett's multiple comparisons test against BEAS-2B; data are presented as mean ± SEM.

Compared with BEAS-2B cells, hsa-miR-9-5p expression was markedly increased in both NSCLC cell lines. The A549 cells showed a 3.56-fold increase, whereas H1299 cells showed a 6.92-fold increase. Both differences were statistically significant compared with BEAS-2B ($p < 0.001$), as shown in Figure 1a.

In contrast, hsa-let-7a-5p expression was reduced in both A549 and H1299 cells. Relative to BEAS-2B cells, hsa-let-7a-5p decreased to 0.36 in A549 and to 0.22 in H1299. Both reductions were statistically significant compared with BEAS-2B ($p < 0.001$), as shown in Figure 1b.

Together, these findings indicate an opposing basal miRNA expression profile in NSCLC cells, characterized by upregulation of the oncogenic miRNA hsa-miR-9-5p and downregulation of the tumor-suppressive hsa-let-7a-5p.

Basal expression of ARID1A, NFAT5, and ZFP36 in NSCLC cell lines

The expression levels of three candidate mRNA targets, ARID1A, NFAT5, and ZFP36, were next analyzed in the same three cell lines. The GAPDH was used as the endogenous control for mRNA normalization, and BEAS-2B was used as the calibrator.

The ARID1A expression was decreased in both NSCLC cell lines compared with BEAS-2B. A549 cells showed a pronounced reduction, with ARID1A expression decreasing to 0.15. H1299 cells also showed reduced ARID1A expression, although the decrease was less

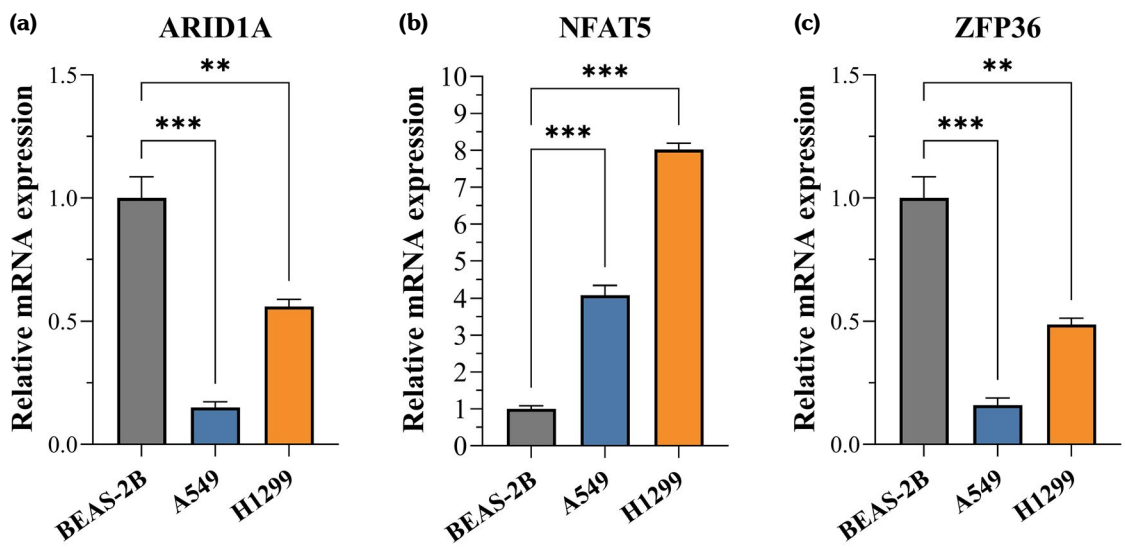

Figure 2. Relative mRNA expression levels of ARID1A, NFAT5, and ZFP36 in BEAS-2B, A549, and H1299 cells. Relative expression levels of ARID1A **(a)**, NFAT5 **(b)**, and ZFP36 **(c)** were determined by qRT-PCR. The GAPDH was used as the endogenous control, and BEAS-2B cells were used as the calibrator. Relative expression was calculated using the 2^-ΔΔCt method. The ARID1A and ZFP36 expression levels were decreased in A549 and H1299 cells compared with BEAS-2B, whereas NFAT5 expression was markedly increased in both cancer cell lines.

Data are presented as mean ± SEM. Statistical comparisons were performed using one-way ANOVA followed by Dunnett's multiple comparisons test against BEAS-2B. ** $p < 0.01$, *** $p < 0.001$ *vs.* BEAS-2B.

marked, with a relative expression level of 0.56. ARID1A expression was therefore suppressed in both NSCLC cell models, particularly in A549 cells, as shown in Figure 2a.

In contrast, NFAT5 expression was strongly increased in both cancer cell lines. The A549 cells exhibited a 4.04-fold increase, whereas H1299 cells showed an 8.02-fold increase compared with BEAS-2B. The induction was more prominent in H1299 cells, indicating that NFAT5 is highly expressed in both NSCLC models examined, as shown in Figure 2b.

The ZFP36 expression was also reduced in both NSCLC cell lines. A549 cells showed a marked decrease to 0.15, while H1299 cells showed a moderate decrease to 0.49

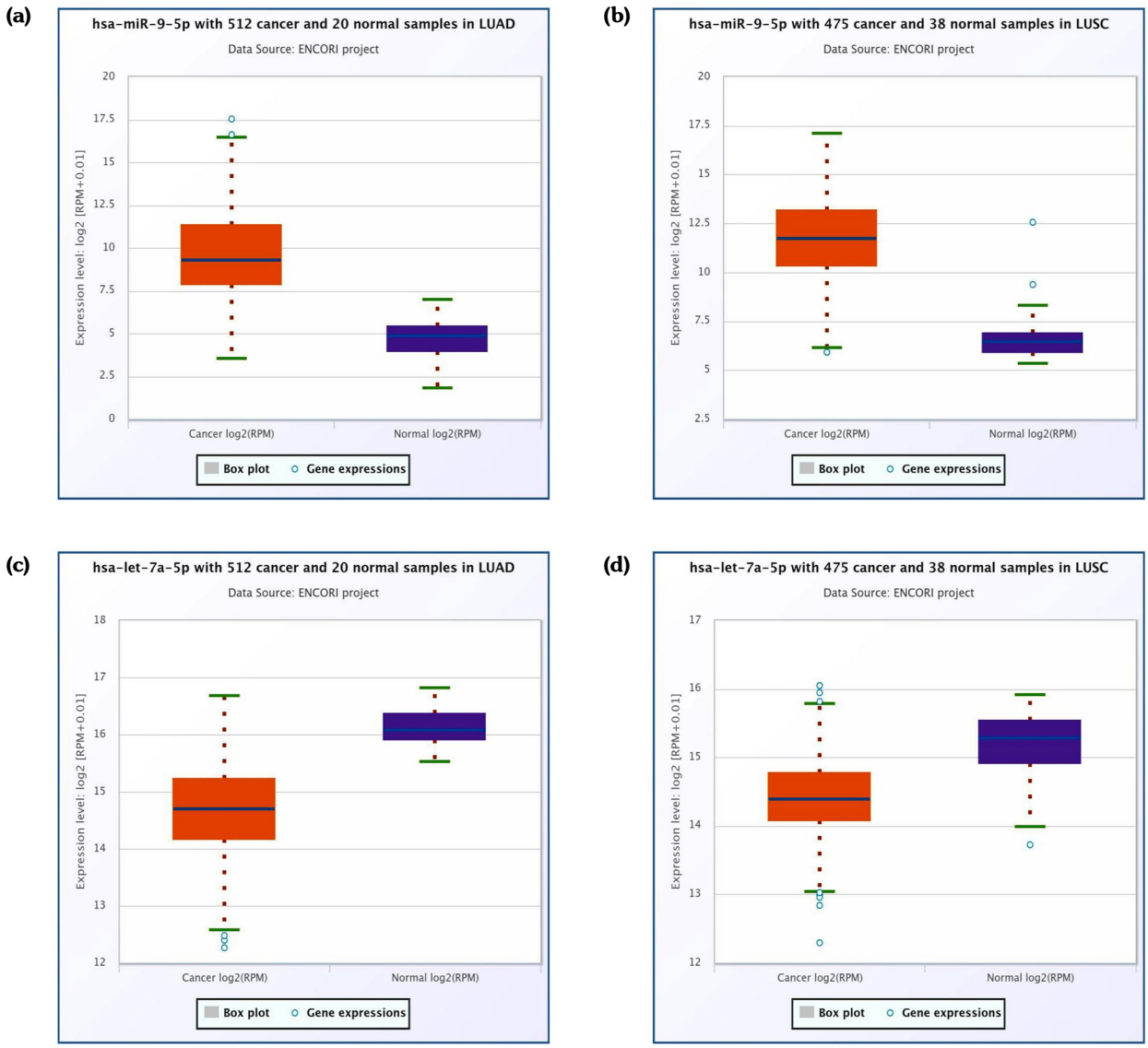

Figure 3. ENCORI/starBase-based tumor-normal expression profiles of hsa-miR-9-5p and hsa-let-7a-5p in LUAD and LUSC cohorts. Tumor-normal expression profiles of hsa-miR-9-5p and hsa-let-7a-5p were evaluated using the ENCORI/starBase Pan-Cancer Analysis Platform. The hsa-miR-9-5p expression was examined in LUAD **(a)** and LUSC **(b)**, whereas hsa-let-7a-5p expression was examined in LUAD **(c)** and LUSC **(d)**. The hsa-miR-9-5p showed higher expression in tumor samples compared with normal samples in both LUAD and LUSC, while hsa-let-7a-5p showed lower expression in tumor samples. The miRNA expression values are presented as log2(RPM + 0.01), as provided by ENCORI/starBase.

LUAD, lung adenocarcinoma, LUSC, lung squamous cell carcinoma.

relative to BEAS-2B. These findings support a reduced basal expression pattern of ZFP36 in NSCLC cells, consistent with its proposed tumor-suppressive role, as shown in Figure 2c.

Integrated miRNA-mRNA expression pattern

Overall, the qRT-PCR results revealed a coordinated expression pattern in A549 and H1299 cells relative to BEAS-2B. Both NSCLC cell lines displayed increased hsa-miR-9-5p and NFAT5 expression, together with reduced hsa-let-7a-5p, ARID1A, and ZFP36 expression. This profile was more pronounced in H1299 cells for hsa-miR-9-5p and NFAT5, whereas in A549 cells, ARID1A and ZFP36 were more strongly suppressed. These findings support a basal regulatory pattern in NSCLC cell lines characterized by oncogenic miRNA activation, loss of tumor-suppressive miRNAs, NFAT5 upregulation, and reduced expression of the candidate tumor suppressors ARID1A and ZFP36.

ENCORI/starBase-based external transcriptomic analysis

To determine whether the *in vitro* expression pattern was reflected in larger patient-derived transcriptomic datasets, ENCORI/starBase Pan-Cancer analyses were performed for LUAD and LUSC cohorts.

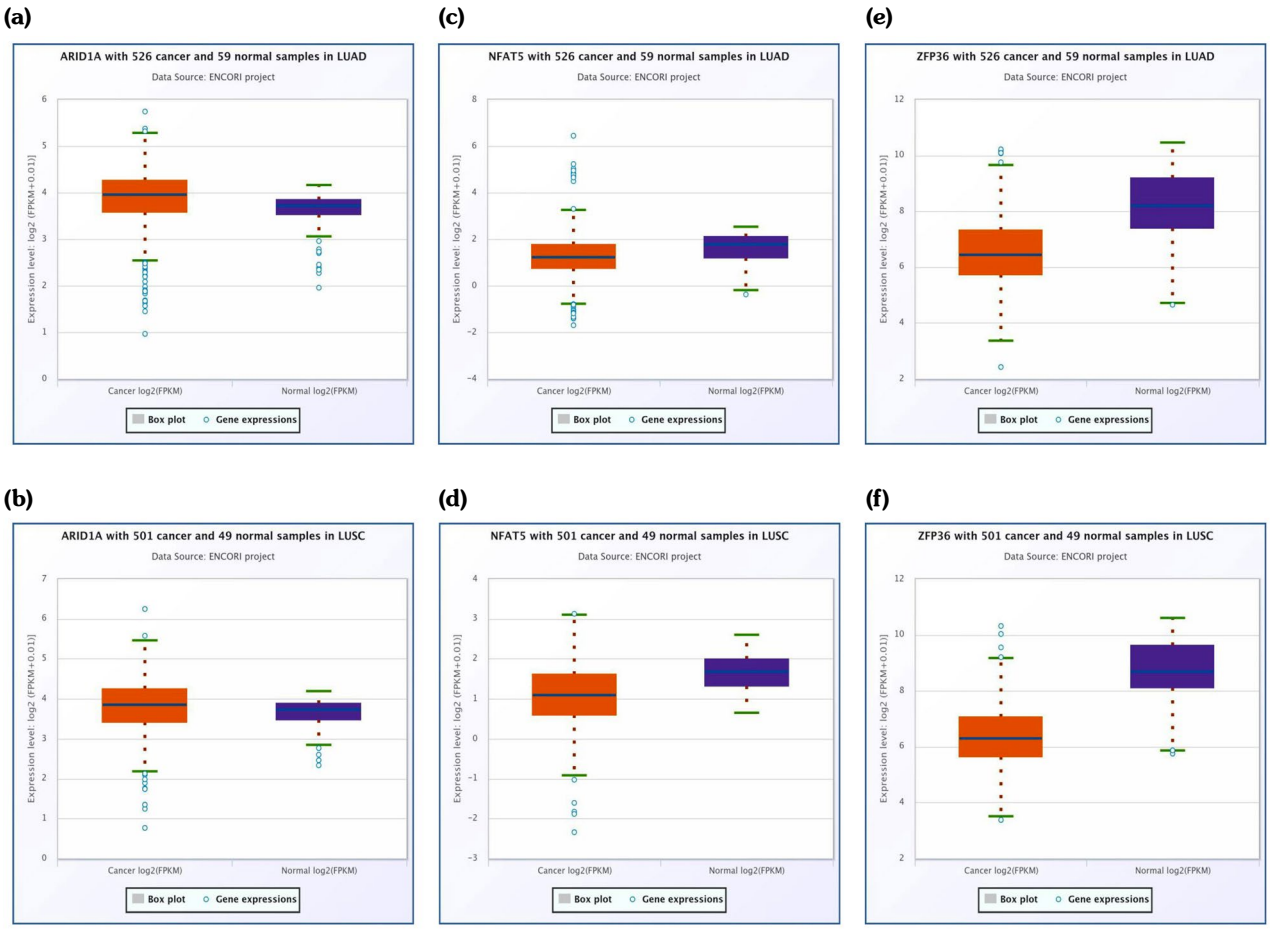

Figure 4. ENCORI/starBase-based tumor-normal expression profiles of ARID1A, NFAT5, and ZFP36 in LUAD and LUSC cohorts. Tumor-normal expression profiles of ARID1A, NFAT5, and ZFP36 were evaluated using the ENCORI/starBase Pan-Cancer Analysis Platform. The ARID1A expression was examined in LUAD **(a)** and LUSC **(b)**, NFAT5 expression in LUAD **(c)** and LUSC **(d)**, and ZFP36 expression in LUAD **(e)** and LUSC **(f)**. The ZFP36 showed lower expression in tumor samples than in normal samples in both LUAD and LUSC. In contrast, ARID1A and NFAT5 showed more complex tumor-normal expression patterns that were not fully concordant with the in vitro qRT-PCR findings. Gene expression values are presented as log2(FPKM + 0.01), as provided by ENCORI/starBase.

LUAD, lung adenocarcinoma, LUSC, lung squamous cell carcinoma.

Tumor-normal expression analyses showed that hsa-miR-9-5p expression was higher in cancer samples than in normal samples in both LUAD and LUSC, as shown in Figures 3a, b. In contrast, hsa-let-7a-5p expression was lower in cancer samples compared with normal samples in both LC subtypes, as shown in Figures 3c, d. These patterns were directionally consistent with the qRT-PCR results showing increased hsa-miR-9-5p and reduced hsa-let-7a-5p expression in A549 and H1299 cells relative to BEAS-2B.

ARID1A and NFAT5 did not show fully concordant tumor–normal expression patterns with the *in vitro* results, as shown in Figures 4a-d. In contrast, among the mRNAs analyzed, ZFP36 showed a lower expression pattern in tumor samples than in normal samples in both LUAD and LUSC cohorts, as shown in Figures 4e, f. This finding was directionally consistent with the reduced ZFP36 expression observed in both NSCLC cell lines.

To further explore potential miRNA-mRNA relationships, ENCORI/starBase co-expression analyses were performed for hsa-miR-9-5p and hsa-let-7a-5p against ARID1A, NFAT5, and ZFP36 in LUAD and LUSC cohorts. Among the analyzed pairs, the most coherent external support was observed for the hsa-miR-9-5p/ZFP36 relationship.

The hsa-miR-9-5p did not show a consistent inverse relationship with ARID1A or NFAT5. In LUAD, hsa-miR-9-5p showed no significant

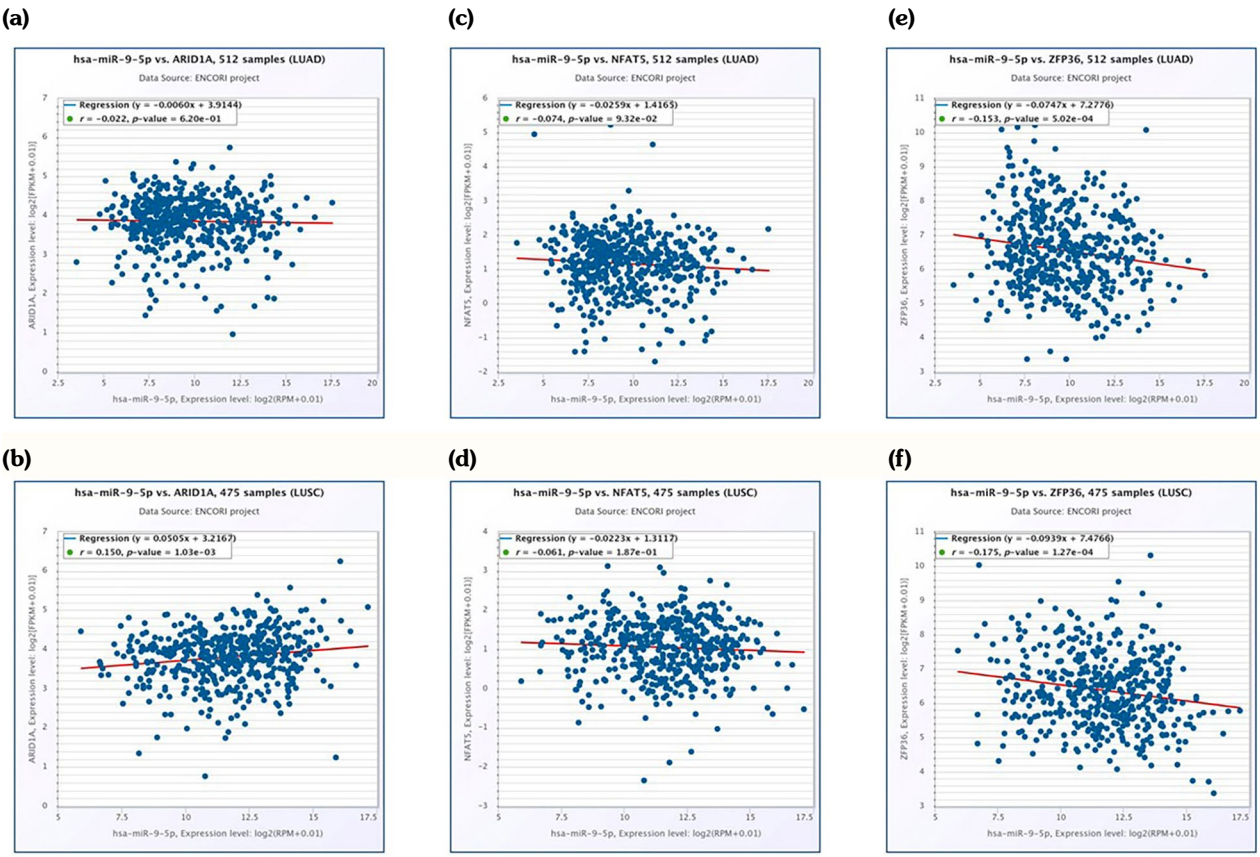

Figure 5. ENCORI/starBase-based co-expression analysis between hsa-miR-9-5p and ARID1A, NFAT5, and ZFP36 in LUAD and LUSC cohorts. Co-expression relationships between hsa-miR-9-5p and the candidate mRNAs were evaluated using ENCORI/starBase. The hsa-miR-9-5p was analyzed against ARID1A in LUAD **(a)** and LUSC **(b)**, NFAT5 in LUAD **(c)** and LUSC **(d)**, and ZFP36 in LUAD **(e)** and LUSC **(f)**. hsa-miR-9-5p showed a weak but statistically significant negative correlation with ZFP36 in both LUAD and LUSC, whereas no consistent inverse relationship was observed with ARID1A or NFAT5. Correlation coefficients and p-values were obtained directly from ENCORI/starBase. miRNA expression values are shown as log2(RPM + 0.01), and mRNA expression values are shown as log2(FPKM + 0.01).
LUAD, lung adenocarcinoma, LUSC, lung squamous cell carcinoma.

correlation with ARID1A (r = –0.022, p = 0.620) or NFAT5 (r = –0.074, p = 0.0932), as shown in Figures 5a and c. In LUSC, hsa-miR-9-5p showed a weak positive correlation with ARID1A (r = 0.150, $p = 1.03 \times 10^{-3}$), whereas its correlation with NFAT5 was not statistically significant (r = –0.061, p = 0.187), as shown in Figures 5b and d. These results do not support a consistent inverse miR-9-5p-associated expression pattern for ARID1A or NFAT5 at the bulk tumor level. The hsa-miR-9-5p showed a weak but statistically significant negative correlation with ZFP36 in both LUAD (r = –0.153, $p = 5.02 \times 10^{-4}$) and LUSC (r = –0.175, $p = 1.27 \times 10^{-4}$), as shown in Figures 5e and f. This inverse relationship was directionally compatible with the *in vitro* pattern of increased hsa-miR-9-5p and reduced ZFP36 expression.

hsa-let-7a-5p showed no significant correlation with ARID1A in LUAD (r = 0.016, p = 0.712), whereas a weak positive correlation was observed in LUSC (r = 0.213, $p = 2.97 \times 10^{-6}$), as shown in Figures 6a and b. Similarly, hsa-let-7a-5p showed no significant correlation with NFAT5 in LUAD (r = 0.058, p = 0.192), but a weak positive correlation was observed in LUSC (r = 0.183, $p = 5.95 \times 10^{-5}$), as shown in Figures 6c and d. For hsa-let-7a-5p, weak positive correlations were observed with ZFP36 in both LUAD (r = 0.127, $p = 3.99 \times 10^{-3}$) and

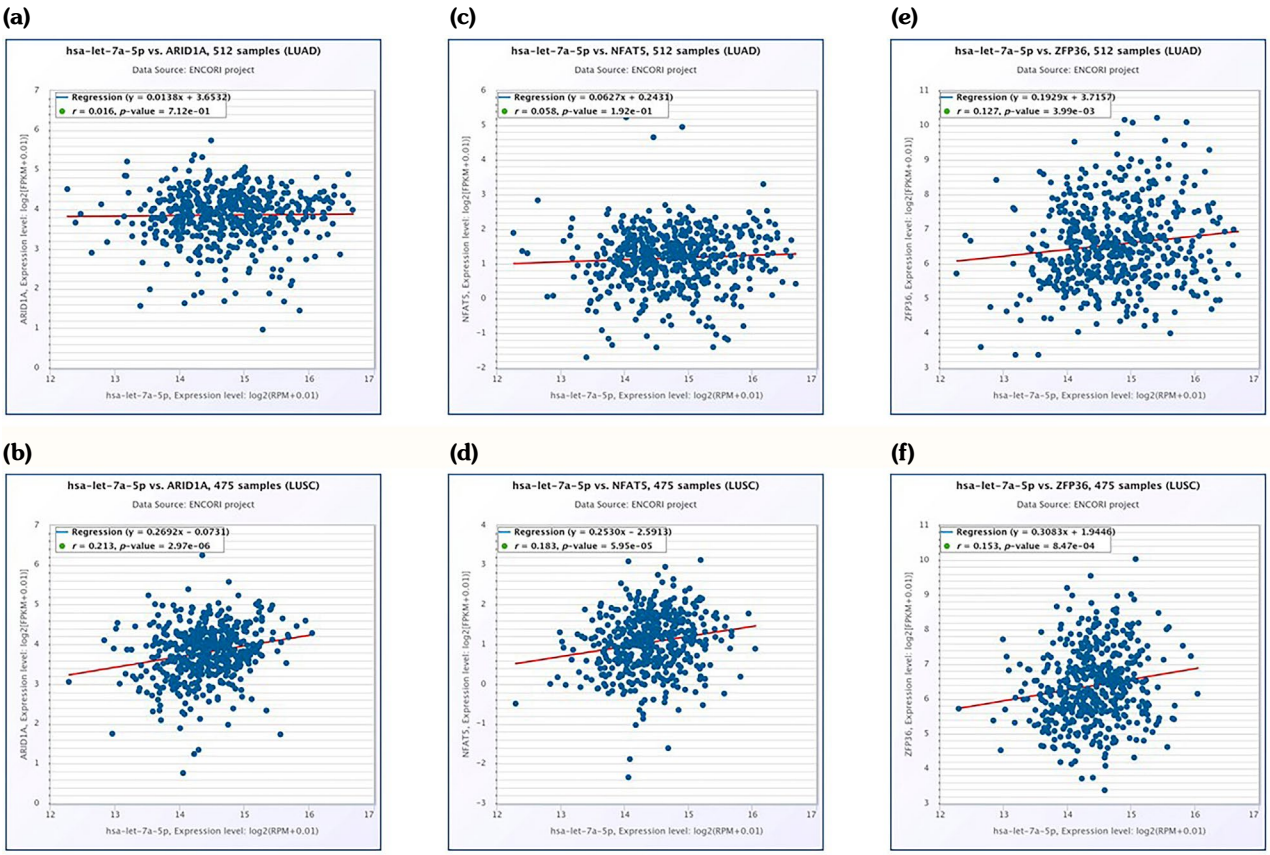

Figure 6. ENCORI/starBase-based co-expression analysis between hsa-let-7a-5p and ARID1A, NFAT5, and ZFP36 in LUAD and LUSC cohorts. Co-expression relationships between hsa-let-7a-5p and the candidate mRNAs were evaluated using ENCORI/starBase. The hsa-let-7a-5p was analyzed against ARID1A in LUAD **(a)** and LUSC **(b)**, NFAT5 in LUAD **(c)** and LUSC **(d)**, and ZFP36 in LUAD **(e)** and LUSC **(f)**. The hsa-let-7a-5p showed weak positive correlations with ZFP36 in both LUAD and LUSC. Positive correlations with ARID1A and NFAT5 were observed only in LUSC, whereas no significant correlations were observed for these pairs in LUAD. Correlation coefficients and p-values were obtained directly from ENCORI/starBase. miRNA expression values are shown as log2(RPM + 0.01), and mRNA expression values are shown as log2(FPKM + 0.01).

LUAD, lung adenocarcinoma, LUSC, lung squamous cell carcinoma.

LUSC ($r = 0.153$, $p = 8.47 \times 10^{-4}$), as shown in Figures 6e and f.

Taken together, ENCORI/starBase analyses partially supported and externally contextualized the *in vitro* qRT-PCR findings. The strongest concordance was observed for increased hsa-miR-9-5p, reduced hsa-let-7a-5p, reduced ZFP36, and the inverse hsa-miR-9-5p/ZFP36 co-expression pattern. However, the ARID1A and NFAT5 results appeared more context-dependent and did not fully mirror the cell culture findings at the bulk tumor transcriptomic level. Therefore, the ENCORI/starBase results were interpreted as supportive and hypothesis-generating rather than confirmatory evidence of direct miRNA-mRNA regulation.

DISCUSSION

In the present study, basal expression profiles of hsa-miR-9-5p, hsa-let-7a-5p, NFAT5, ARID1A, and ZFP36 were evaluated in BEAS-2B, A549, and H1299 cells. The main finding was a coordinated expression pattern in NSCLC cell lines characterized by increased hsa-miR-9-5p and NFAT5 expression together with reduced hsa-let-7a-5p, ARID1A, and ZFP36 expression, relative to the non-tumorigenic bronchial epithelial reference BEAS-2B. This profile suggests a putative regulatory pattern in which oncogenic miRNA activation, tumor-suppressive miRNA loss, stress-responsive transcriptional activation, and reduced tumor-suppressive mRNA expression coexist in NSCLC cell models. Since the present study is based on basal expression profiling, these findings are interpreted as association-level evidence rather than direct proof of miRNA-mRNA regulation.

The upregulation of hsa-miR-9-5p in A549 and H1299 cells is consistent with previous reports describing miR-9-5p as an oncogenic miRNA in NSCLC and LUAD. Li et al.[7] showed that miR-9-5p promotes NSCLC cell proliferation, invasion, and metastasis through repression of TGFBR2, while Zhu et al.[6] demonstrated that miR-9-5p enhances LUAD cell proliferation, migration, and invasion by targeting ID4. More recently, Zhang et al.[8] reported increased miR-9-5p expression in NSCLC tissues and cell lines relative to non-malignant controls, with associations to smoking-related clinicopathological features. The increased miR-9-5p expression observed here in both NSCLC cell lines is therefore compatible with an oncogenic miRNA phenotype, although the functional consequences are likely to depend on cell-line-specific target availability and pathway context.[6-8]

In contrast, hsa-let-7a-5p was decreased in both A549 and H1299 cells compared with BEAS-2B. This finding is consistent with the established tumor-suppressive role of the let-7 family in LC. In a systematic review and meta-analysis, Pop-Bica et al.[20] emphasized the clinical relevance of let-7 family members in NSCLC and discussed their regulatory relationship with oncogenic pathways involving RAS, myelocytomatosis viral oncogene (MYC), high mobility group A (HMGA), signal transducer and activator of transcription 3 (STAT3), and Janus kinase 2 (JAK2). The reduced let-7a-5p expression observed here therefore supports the interpretation that loss of tumor-suppressive miRNA activity may accompany NSCLC-associated transcriptional reprogramming. The concurrent increase in miR-9-5p and reduction in let-7a-5p indicate a reciprocal miRNA profile rather than a single-miRNA alteration.

Among the three candidate mRNA targets, NFAT5 showed the most pronounced increase, particularly in H1299 cells. This finding is biologically meaningful given that NFAT5, also known as TonEBP, is increasingly recognized as a stress-responsive transcription factor involved in tumor progression, metabolic adaptation, inflammation, and therapy resistance. Dou et al.[21] reported that circ_0001944 promotes proliferation, migration, invasion, glycolysis, and tumor growth in NSCLC by upregulating NFAT5 through sequestration of miR-142-5p, supporting the concept that NFAT5 can be regulated by non-coding RNA networks and can contribute to malignant phenotypes in NSCLC.

The relevance of NFAT5 in LC is further supported by recent evidence linking TonEBP and NFAT5 to macrophage-induced cisplatin resistance, migration, and invasion in A549 cells. Song et al.[22] showed that macrophage-conditioned medium increased TonEBP and NFAT5 expression, enhanced

cisplatin resistance and motility, and that RNA interference-mediated suppression of TonEBP and NFAT5 reduced cisplatin resistance, migration, and invasion. These findings place NFAT5 at the intersection of tumor microenvironment interaction, inflammatory signaling, drug resistance, and invasive behavior. The increased NFAT5 expression detected in A549 and H1299 cells in the present study may therefore reflect a stress-adaptive and potentially pro-tumorigenic transcriptional state, although this interpretation remains speculative within the present dataset.

The relationship between the two miRNAs and NFAT5 requires cautious interpretation. The reduction of hsa-let-7a-5p together with increased NFAT5 is directionally consistent with loss of tumor-suppressive miRNA-mediated repression of a pro-tumorigenic factor. However, the simultaneous increase in hsa-miR-9-5p and NFAT5 does not support a simple direct inhibitory relationship between miR-9-5p and NFAT5 under basal conditions. This apparent discrepancy may reflect indirect regulation, dominant transcriptional activation, circRNA-mediated derepression as previously demonstrated for NFAT5 in NSCLC,[21] or stress-related pathway activation overriding potential miRNA repression. Within the present dataset, the let-7a-5p and NFAT5 relationship therefore appears more directionally coherent than a direct miR-9-5p and NFAT5 suppressive model.

The ARID1A expression was reduced in both NSCLC cell lines, with a stronger decrease in A549 cells. This is compatible with the tumor-suppressive role of ARID1A as a core component of the SWI/SNF chromatin-remodeling complex. Recent translational data further support the clinical relevance of ARID1A loss in LUAD. Yang et al.,[23] reported that ARID1A deficiency attenuates response to EGFR-tyrosine kinase inhibitor treatment in EGFR-mutant LUAD, with loss of ARID1A expression linked to EGFR-related signaling activation. Reduced ARID1A expression in A549 and H1299 cells may therefore reflect loss of chromatin-dependent tumor-suppressive regulation with potential implications for metastatic behavior and therapy resistance.

The relationship between miRNA changes and ARID1A expression should not be overinterpreted. The combination of increased hsa-miR-9-5p and reduced ARID1A is directionally compatible with an oncogenic miRNA-associated suppression model, but direct binding of miR-9-5p to the ARID1A 3'UTR has not been established in NSCLC and was not tested here. In contrast, reduced hsa-let-7a-5p would not explain ARID1A downregulation through a simple direct targeting mechanism, since decreased let-7a-5p would be expected to relieve repression of its direct targets. The ARID1A downregulation in these NSCLC cell lines may therefore involve additional mechanisms, including genetic alteration, epigenetic regulation, transcriptional repression, protein stability changes, or regulation by other non-coding RNAs.[24] Direct testing is required before ARID1A can be assigned as a functional downstream target of either miR-9-5p or let-7a-5p in this model.

The ZFP36 was also reduced in both A549 and H1299 cells. The ZFP36, also known as tristetraprolin, is an AU-rich element-binding RNA-binding protein that promotes mRNA decay and is broadly considered a tumor-suppressive post-transcriptional regulator. Saini et al.,[16] reviewed the tristetraprolin family and highlighted that TTP family RNA-binding proteins regulate multiple cancer-relevant traits, including inflammation, proliferation, metastasis, prognosis, and chemotherapy response. Reduced ZFP36 expression may therefore create a permissive post-transcriptional environment by stabilizing transcripts that would normally be degraded.

In NSCLC specifically, Zhang et al.[17] demonstrated that ZFP36 mediates BARX1 mRNA destabilization. Loss of ZFP36 increased BARX1 expression and promoted proliferation, migration, invasion, and tumorigenicity through activation of oncogenic programs involving CDC20, CDC45, TRIM37, and MMP-9. The reduction of ZFP36 observed in the present study is therefore consistent with a model in which NSCLC cells may lose an important mRNA decay checkpoint, potentially facilitating oncogenic transcript stabilization. This interpretation is particularly relevant since ZFP36 represents

a regulatory layer distinct from both miRNA repression and chromatin remodeling.

Taken together, the present expression pattern suggests two biologically plausible regulatory interpretations. First, hsa-miR-9-5p upregulation, together with ARID1A and ZFP36 downregulation, is compatible with an oncogenic miRNA-associated reduction of tumor-suppressive regulatory layers, namely chromatin remodeling and mRNA decay. Second, hsa-let-7a-5p downregulation together with NFAT5 upregulation is compatible with loss of tumor-suppressive miRNA constraint on a pro-tumorigenic transcription factor. This framework is biologically attractive since NFAT5, ARID1A, and ZFP36 represent three mechanistically distinct levels of gene regulation: stress-responsive transcriptional signaling, chromatin remodeling, and post-transcriptional mRNA turnover. Nevertheless, the current data cannot determine whether these relationships are direct, indirect, or parallel consequences of broader NSCLC-associated reprogramming.

To further evaluate whether the *in vitro* expression pattern reflects findings observable in larger patient-derived datasets, ENCORI/starBase Pan-Cancer analyses were performed in LUAD and LUSC cohorts. The most robust concordance between the cell culture findings and the cohort-level data was observed for hsa-miR-9-5p, hsa-let-7a-5p, and ZFP36. Higher hsa-miR-9-5p and lower hsa-let-7a-5p expression in tumor samples relative to normal lung tissue in both LUAD and LUSC supports the *in vitro* miRNA expression profile and is consistent with previous reports describing miR-9-5p as oncogenic and let-7 family members as tumor-suppressive in LC.[5,9,20] Similarly, ZFP36 expression was reduced in tumor samples in both LUAD and LUSC, directionally consistent with the reduction observed in A549 and H1299 cells and with the post-transcriptional tumor-suppressive role of ZFP36 in NSCLC.[16,17]

In contrast, ARID1A and NFAT5 did not show fully concordant tumor-normal expression patterns at the bulk tumor level. Whereas both cell lines exhibited reduced ARID1A and increased NFAT5 expression relative to BEAS-2B, the ENCORI/starBase cohort distributions suggested more complex subtype-dependent profiles. Several factors may account for this discrepancy. First, BEAS-2B is an SV40 large T antigen-immortalized bronchial epithelial line and may not fully recapitulate the transcriptomic profile of adjacent normal lung tissue used as the cohort reference.[25] Second, bulk tumor expression averages across heterogeneous cell populations, including tumor cells, stromal cells, and immune infiltrate, whereas the *in vitro* signal reflects tumor cell-autonomous expression. Third, ARID1A inactivation in LUAD is frequently genetic, with mutation or copy-number alteration accounting for functional loss in the absence of strict mRNA-level reduction.[15,24] For NFAT5, stress-responsive expression depends on osmotic, hypoxic, and inflammatory cues that vary substantially between tightly controlled *in vitro* conditions and patient tumor microenvironments.[21,22] Therefore, the *in vitro* ARID1A and NFAT5 alterations are interpreted as cell-line-specific expression changes requiring independent validation rather than as universally conserved tumor-level signatures.

Co-expression analyses provided a partial but informative external context. Among the six miRNA-mRNA pairs examined, the hsa-miR-9-5p and ZFP36 relationship showed the most consistent inverse association, with weak but statistically significant negative correlations in both LUAD ($r = -0.153$, $p = 5.02 \times 10^{-4}$) and LUSC ($r = -0.175$, $p = 1.27 \times 10^{-4}$). This pattern is directionally compatible with an oncogenic miR-9-5p contribution to ZFP36 suppression in NSCLC, although direct binding has not been demonstrated and the correlation strength precludes definitive causal interpretation. No consistent inverse correlations were detected between hsa-miR-9-5p and ARID1A or NFAT5 at the bulk tumor level. For hsa-let-7a-5p, weak but significant positive correlations were observed with ZFP36 in both LUAD and LUSC, as well as with ARID1A and NFAT5 in LUSC. These positive correlations are unlikely to reflect direct miRNA-mediated regulation, which would predict inverse rather than positive associations. A more plausible interpretation is that hsa-let-7a-5p, ARID1A,

and ZFP36 are coordinately downregulated in tumor samples as part of a broader tumor-suppressive program; cohort-level correlation then captures their co-suppression rather than a direct regulatory link. Therefore, the ENCORI/starBase results are best interpreted as supportive and hypothesis-generating, with the hsa-miR-9-5p and ZFP36 axis emerging as the most coherent candidate for future mechanistic validation through 3'UTR luciferase reporter assays and miRNA mimic and inhibitor experiments.

The differences between A549 and H1299 cells are also informative. The H1299 cells showed stronger induction of hsa-miR-9-5p and NFAT5, whereas A549 cells showed more pronounced suppression of ARID1A and ZFP36. This suggests that the proposed signature is not uniform across NSCLC cell models and may be influenced by cell-line-specific genetic background, differentiation state, signaling dependencies, and stress-response programs. A relevant example is tumor protein p53 (TP53) status: A549 retains wild-type p53, whereas H1299 carries a homozygous TP53 deletion and is p53-null.[26] Such genetic differences may shape downstream miRNA and mRNA expression profiles in distinct ways. Although both A549 and H1299 showed the same overall direction of change, these findings should not be generalized to all NSCLC subtypes without validation in additional LUAD and non-LUAD cell lines and in patient-derived tumor samples.

The use of BEAS-2B as the reference cell line also requires methodological qualification. BEAS-2B is widely used as a non-tumorigenic bronchial epithelial reference model, but it is an immortalized cell line rather than a primary normal bronchial epithelial cell. Han et al.[25] reported that BEAS-2B cells are SV40 large T antigen-expressing, non-tumorigenic cells with features that complicate their interpretation as a purely normal epithelial model. BEAS-2B is therefore appropriate as an initial non-malignant bronchial epithelial comparator, but validation using primary normal human bronchial epithelial cells or additional non-malignant bronchial epithelial models would strengthen translational interpretation.

Several limitations of the present study should be considered when interpreting the findings. First, the analyses were based on basal expression profiling in a limited number of NSCLC cell lines and may therefore not fully capture the biological heterogeneity of NSCLC in clinical settings. In addition, the study focused on transcript-level alterations and did not include protein-level validation experiments. Although ENCORI/starBase analyses provided supportive external evidence, the observed miRNA-mRNA correlations were generally weak and should be interpreted cautiously, since statistically significant associations in large transcriptomic cohorts do not necessarily indicate direct or biologically meaningful regulatory interactions. Furthermore, functional validation experiments such as luciferase reporter assays, miRNA mimic/inhibitor transfection, or knockdown studies were not performed. Therefore, the findings of the present study should be regarded as association-based and hypothesis-generating rather than definitive evidence of direct miRNA-mRNA regulation. Additional studies incorporating functional assays, protein-level analyses, and broader NSCLC models will be necessary to further clarify the biological significance of the proposed expression patterns.

In conclusion, the present study identifies a basal expression pattern in NSCLC cell lines characterized by hsa-miR-9-5p upregulation, hsa-let-7a-5p downregulation, NFAT5 upregulation, and reduced ARID1A and ZFP36 expression. This profile is compatible with a putative miRNA-mRNA regulatory signature involving oncogenic miRNA activation, tumor-suppressive miRNA loss, stress-responsive transcriptional activation, chromatin-regulatory loss, and impaired mRNA decay control. Although direct regulatory interactions remain to be validated, these findings provide a rational basis for future mechanistic studies investigating the hsa-miR-9-5p and hsa-let-7a-5p axis in relation to NFAT5, ARID1A, and ZFP36 in NSCLC biology.

Data Sharing Statement: The data that support the findings of this study are available from the corresponding author upon reasonable request.

Author Contributions: Y.T.K., P.Y.U.: Conception, analysis, drafting.

Conflict of Interest: The authors declared no conflicts of interest with respect to the authorship and/or publication of this article.

Funding: The authors received no financial support for the research and/or authorship of this article.

AI Disclosure: The authors declare that artificial intelligence (AI) tools were not used, or were used solely for language editing, and had no role in data analysis, interpretation, or the formulation of conclusions. All scientific content, data interpretation, and conclusions are the sole responsibility of the authors. The authors further confirm that AI tools were not used to generate, fabricate, or 'hallucinate' references, and that all references have been carefully verified for accuracy.

REFERENCES

1. Bray F, Laversanne M, Sung H, Ferlay J, Siegel RL, Soerjomataram I, et al. Global cancer statistics 2022: GLOBOCAN estimates of incidence and mortality worldwide for 36 cancers in 185 countries. CA Cancer J Clin 2024;74:229-63. doi: 10.3322/caac.21834.
2. Xiang Y, Liu X, Wang Y, Zheng D, Meng Q, Jiang L, Yang et al. Mechanisms of resistance to targeted therapy and immunotherapy in non-small cell lung cancer: Promising strategies to overcoming challenges. Front Immunol 2024;15:1366260. doi: 10.3389/fimmu.2024.1366260.
3. Bartel DP. Metazoan MicroRNAs. Cell 2018;173:20-51. doi: 10.1016/j.cell.2018.03.006.
4. Calin GA, Croce CM. MicroRNA signatures in human cancers. Nat Rev Cancer 2006;6:857-66. doi: 10.1038/nrc1997.
5. Inamura K. Diagnostic and therapeutic potential of microRNAs in lung cancer. Cancers (Basel) 2017;9:49. doi: 10.3390/cancers9050049.
6. Zhu K, Lin J, Chen S, Xu Q. miR-9-5p promotes lung adenocarcinoma cell proliferation, migration and invasion by targeting ID4. Technol Cancer Res Treat 2021;20:15330338211048592. doi: 10.1177/15330338211048592.
7. Li G, Wu F, Yang H, Deng X, Yuan Y. MiR-9-5p promotes cell growth and metastasis in non-small cell lung cancer through the repression of TGFBR2. Biomed Pharmacother 2017;96:1170-8. doi: 10.1016/j.biopha.2017.11.105.
8. Zhang TX, Duan XC, Cui Y, Zhang Y, Gu M, Wang ZY, et al. Clinical significance of miR-9-5p in NSCLC and its relationship with smoking. Front Oncol 2024;14:1376502. doi: 10.3389/fonc.2024.1376502.
9. Takamizawa J, Konishi H, Yanagisawa K, Tomida S, Osada H, Endoh H, et al. Reduced expression of the let-7 microRNAs in human lung cancers in association with shortened postoperative survival. Cancer Res 2004;64:3753-6. doi: 10.1158/0008-5472.CAN-04-0637.
10. Johnson SM, Grosshans H, Shingara J, Byrom M, Jarvis R, Cheng A, et al. RAS is regulated by the let-7 microRNA family. Cell 2005;120:635-47. doi: 10.1016/j.cell.2005.01.014.
11. Kumar MS, Erkeland SJ, Pester RE, Chen CY, Ebert MS, Sharp PA, et al. Suppression of non-small cell lung tumor development by the let-7 microRNA family. Proc Natl Acad Sci U S A 2008;105:3903-8. doi: 10.1073/pnas.0712321105.
12. Guo K, Jin F. NFAT5 promotes proliferation and migration of lung adenocarcinoma cells in part through regulating AQP5 expression. Biochem Biophys Res Commun 2015;465:644-9. doi: 10.1016/j.bbrc.2015.08.078.
13. Chen J, Mei T, Wang J, Qin T, Huang D. NFAT5 regulates IL8 to promote cell growth and migration in non-small cell lung cancer. Thorac Cancer 2025;16:e70166. doi: 10.1111/1759-7714.70166.
14. Sun D, Zhu Y, Zhao H, Bian T, Li T, Liu K, et al. Loss of ARID1A expression promotes lung adenocarcinoma metastasis and predicts a poor prognosis. Cell Oncol (Dordr) 2021;44:1019-34. doi: 10.1007/s13402-021-00616-x.
15. Sun D, Feng F, Teng F, Xie T, Wang J, Xing P, et al. Multiomics analysis revealed the mechanisms related to the enhancement of proliferation, metastasis and EGFR-TKI resistance in EGFR-mutant LUAD with ARID1A deficiency. Cell Commun Signal 2023;21:48. doi: 10.1186/s12964-023-01065-9.
16. Saini Y, Chen J, Patial S. The tristetraprolin family of RNA-binding proteins in cancer: Progress and future prospects. Cancers (Basel) 2020;12:1539. doi: 10.3390/cancers12061539.
17. Zhang T, Qiu L, Cao J, Li Q, Zhang L, An G, et al. ZFP36 loss-mediated BARX1 stabilization promotes malignant phenotypes by transactivating master oncogenes in NSCLC. Cell Death Dis 2023;14:527. doi: 10.1038/s41419-023-06044-z.
18. Li JH, Liu S, Zhou H, Qu LH, Yang JH. starBase v2.0: Decoding miRNA-ceRNA, miRNA-ncRNA and protein-RNA interaction networks from large-scale CLIP-Seq data. Nucleic Acids Res 2014;42(Database issue):D92-7. doi: 10.1093/nar/gkt1248.
19. Livak KJ, Schmittgen TD. Analysis of relative gene expression data using real-time quantitative PCR and the 2(-Delta Delta C(T)) Method. Methods 2001;25:402-8. doi: 10.1006/meth.2001.1262.
20. Pop-Bica C, Pintea S, Magdo L, Cojocneanu R, Gulei D, Ferracin M, et al. The clinical utility of miR-21 and let-7 in Non-Small Cell Lung Cancer (NSCLC). A systematic review and meta-analysis. Front Oncol 2020;10:516850. doi: 10.3389/fonc.2020.516850.
21. Dou Y, Tian W, Wang H, Lv S. Circ_0001944 contributes to glycolysis and tumor growth by

upregulating NFAT5 through acting as a decoy for miR-142-5p in non-small cell lung cancer. Cancer Manag Res 2021;13:3775-87. doi: 10.2147/CMAR.S302814.

22. Song HJ, Kim YH, Choi HN, Kim T, Kim SJ, Kang MW, et al. TonEBP/NFAT5 expression is associated with cisplatin resistance and migration in macrophage-induced A549 cells. BMC Mol Cell Biol 2024;25:6. doi: 10.1186/s12860-024-00502-y.
23. Yang F, Hou H, Wang G, Fu G, Huo X, Duan X, et al. ARID1A deficiency attenuates the response to EGFR-TKI treatment in lung adenocarcinoma. Front Pharmacol 2025;16:1582005. doi: 10.3389/fphar.2025.1582005.
24. Mathur R. ARID1A loss in cancer: Towards a mechanistic understanding. Pharmacol Ther 2018;190:15-23. doi: 10.1016/j.pharmthera.2018.05.001.
25. Han X, Na T, Wu T, Yuan BZ. Human lung epithelial BEAS-2B cells exhibit characteristics of mesenchymal stem cells. PLoS One 2020;15:e0227174. doi: 10.1371/journal.pone.0227174.
26. Mitsudomi T, Steinberg SM, Nau MM, Carbone D, D'Amico D, Bodner S, et al. P53 gene mutations in non-small-cell lung cancer cell lines and their correlation with the presence of ras mutations and clinical features. Oncogene 1992;7:171-80.